[UCI]I804:24011-200000266531

2018 년 2 월

석사학위 논문

The Cytoprotective Role of Sestrin2 by Ferroptosis-mediated Hepatocyte Death

조선대학교 대학원

약 학 과

박 수 정

The Cytoprotective Role of Sestrin2 by Ferroptosis-mediated Hepatocyte Death

Ferroptosis 매개 간세포사멸에서 Sestrin2 의

간세포 보호 효능

2018 년 2 월 23 일

조선대학교 대학원

약 학 과

박 수 정

The Cytoprotective Role of Sestrin2 by Ferroptosis-mediated Hepatocyte Death

지도교수 기 성 환

이 논문을 약학 석사학위신청 논문으로 제출함

2017 년 10 월

조선대학교 대학원

약 학 과

박 수 정

박수정의 석사학위논문을 인준함

위원장 조선대학교 교수 최 홍 석 인

위 원 조선대학교 교수 이 금 화 인

위 원 조선대학교 교수 기 성 환 인

2017 년 11 월

조선대학교 대학원

CONTENTS

CONTENTS.....i

LIST OF FIGURES.....iii

ABBREVIATIONS.....iv

ABSTRACT (Korean)..... v

I. INTRODUCTION.....1

II. MATERIALS AND METHODS.....4

1. Reagents and Antibodies 4
2. Cell culture.....4
3. Establishment of a stable cell line expressing Sestrin2.....4
4. Primary hepatocyte isolation 5
5. MTT assay.....5
6. RNA isolation and RT-PCR analysis 6
7. Plasmid transfection and Luciferase assay 7
8. Immunoblot analysis 7

9. siRNA Knockdown Experiment 8
10. Determination of GSH content 8
11. Measurement of ROS production 8
12. Mito SOX fluorescence analysis.....8
13. Iron assay.....9
14. Lipid peroxidation assay.....9
15. Statistical analysis.....9

III. RESULTS.....10

1. Increased Sestrin2 expression levels during ferroptosis 10
2. Transcriptional regulation of Sestrin2 expression 13
3. Involvement of ROS production in erastin-induced Sestrin2 upregulation ...16
4. The role of Nrf2 activation in Sestrin2 induction by ferroptosis 19
5. The cytoprotective effect of Sestrin2 against ferroptosis 22
6. Schematic diagram.....25

IV. DISCUSSION.....26

V. REFERENCES.....29

LIST OF FIGURES

Figure 1. Increased sestrin2 expression levels by ferroptosis inducers.

Figure 2. Transcriptional regulation of Sestrin2 gene expression.

Figure 3. Involvement of ROS in erastin-induced ferroptosis.

Figure 4. Involvement of Nrf2 activation in erastin-induced Sestrin2 induction.

Figure 5. Sestrin2 overexpression inhibits erastin-induced ferroptosis.

Figure 6. Schematic diagram

ABBREVIATIONS

ActD	Actinomycin-D
BHA	Butylated hydroxyanisole
DCFH-DA	2’,7’-Dichlorofluorescein diacetate
DMSO	Dimethylsulfoxide
DPI	Diphenyleneiodonium chloride
BSO	Buthionine sulfoximine
MTT	3-(4,5-Dimethylthiazol-2-yl)-2,5-diphenyl-tetrazolium bromide
H_2O_2	Hydrogen peroxide
MEF	Mouse embryonic fibroblast
NAC	*N*-acetyl-L-cysteine
Nrf2	NF-E2-related factor 2
ROS	Reactive oxygen species
Fer-1	Ferrostatin-1
Nec-1	Necrostatin-1
DFO	Deferoxamine
ZVAD-FMK	Caspase inhibitor 1
GSH	Glutathione
GPX4	Glutathione peroxidase 4
HCC	Hepatocellular carcinoma
MDA	Malondialdehyde
SESN2	Sestrin2

국 문 초 록

Ferroptosis 매개 간세포사멸에서 Sestrin2 의 간세포 보호 효능

박 수 정

지 도 교 수: 기 성 환

약학과

조선대학교 대학원

Ferroptosis는 glutathione 합성 억제 또는 iron축적에 의한 활성산소 및 부가물이 세포 내에 축적되어 지질과산화 산물의 생성 및 세포 장애를 유발하며 나아가 세포 사를 촉진하게 되는 non-apoptotic한 세포사멸의 형태 중 하나이다. Sestrin2은 DNA 손상, 저산소증, 산화적 스트레스 등을 포함하는 다양한 자극에 의해 활성화되어 항산화 효소로써의 역할을 할 뿐 아니라, 세포보호 작용 및 세포 내 항상성 유지에 기여하는 유전자로 알려져 있다. Sestrin2의 발현 및 활성화 조절을 매개하는 주요 조절인자로는 p53, Nrf2, HIF-1α 등과 같은 스트레스에 의해 매개되어 활성화되는 전사인자가 있다. 그러나, Ferroptosis가 유도되는 상황에서의 Sestrin2의 발현기전 및 역할에 관한 연구는 전무한 상태이다. 본 연구에서

는 erastin, sorafenib 및 buthionine sulfoximine을 포함한 ferroptosis 유도제에 의한 Sestrin2 발현과 ferroptosis 매개 세포 사멸에서 Sestrin2의 보호효능을 연구하였다.

첫 번째로, 간세포에서 Ferroptosis 유도제에 의해 시간과 용량 의존적으로 증가하는 Sestrin2의 단백질 발현을 관찰하였다. 또한, ferroptosis 유도제인 erastin은 Sestrin2의 mRNA와 luciferase의 발현도 증가시켰다. 이것은 ferroptosis 유도제에 의해서 증가되는 Sestrin2의 발현이 전사적인 수준에서부터 조절된다는 것을 의미한다. 다음으로는, erastin이 항산화 효소 발현을 조절하는 마스터 전사인자인 Nrf2를 활성화 할 수 있는지를 확인하였다. Erastin에 의해 Sestrin2 프로모터영역에서 전사인자인 Nrf2와 결합하는 부분 (ARE)의 활성이 증가함을 관찰하였으며, 핵 내 Nrf2의 발현 역시 함께 증가함을 확인하였다. 더욱이, Nrf2의 knockout 과 knockdown 실험에서 erastin에 의한 Sestrin2 발현증가가 상쇄되었으며, Sestrin2 프로모터영역에서 ARE을 결손 시켰을 때도 erastin에 의해 유도되는 Sestrin2의 luciferase 활성이 억제 되었다. 이러한 결과들은 erastin에 의한 Sestrin2발현 증가가 Nrf2/ARE 활성화를 매개함을 시사한다.

두 번째로, ferroptosis 매개 세포 사멸에서 Sestrin2의 보호효능을 Sestrin2가 stable하게 발현되는 간세포주를 활용하여 평가하였다. Sestrin2 과발현 세포주와 대조군 세포주에서 Erastin에 의해 유도되는 세포 사멸 정도를 비교해 본 결과, erastin에 의해 유도되는 세포 사멸이 Sestrin2 과발현 세포주에서유의적으로 억제됨을 관찰하였다. 그리고, eastin에 의한 ROS 및 GSH 고갈 역시 Sestrin2 발현에 의해 거의 완벽하게 감소됨을 확인하였다. 이는 Sestrin2이 erastin에 의해 유

도되는 ferroptosis를 억제함으로 간세포보호 효능을 가지고 있음을 시사한다.

결과적으로, ferroptosis 상황에서 Nrf2 활성화에 의해 Sestrin2 발현이 유도되고, 유도된 Sestrin2가 ferroptosis에 의한 간세포손상을 방어한다. 이는 과잉의 iron축적에 의한 간세포 손상과 이로 인한 간질환에서 Sestrin2이 새로운 치료 표적이 될 수 있음을 제시한다.

I. INTRODUCTION

Iron is required for several specific functions in the body such as oxygen transport, electron transport, and deoxyribonucleic acid (DNA) synthesis (Abbaspour et al., 2014). Thus deficiency in iron can cause anemia and other diseases or health problem. However, excessive amounts of iron can result in tissue damage (Miller et al, 2013). As iron is well known to form free radicals (Blumberg et al, 2004), its concentration in tissues must be tightly regulated for maintaining iron homeostasis (Horowitz et al., 2010). The major target organ for iron toxicity is liver, because it is chiefly responsible for taking up excessive amount of iron from blood stream and storing it. Iron overloads present hepatic toxicities affecting multiple cell types (e.g., hepatocyte, Kupffer cells, and hepatic stellate cells) and multiple subcellular organelles (smooth endoplasmic reticulum, mitochondria, and lysosome) (Deugnier et al., 2011). Iron overload is also relatively common in alcoholic liver disease, nonalcoholic fatty liver disease, and chronic hepatitis C virus. Moreover, 30% of patients with end-stage liver disease such as liver cirrhosis and hepatocellular carcinoma (HCC) have elevated serum iron levels (Abbaspour, et al., 2014).

Iron accumulation plays a major role in the development and progress of ferroptosis, a newly identified form of regulated non-apoptotic cell death (Latunde-Dada, 2017). Ferroptosis is characterized by overwhelming iron-dependent accumulation of lethal levels of lipid peroxidation products (Xie et al., 2016). It has been reported that deficiency of intracellular cysteine by suppressing a specific light-chain subunit of the cysteine/glutamate antiporter (SLC7A11, or system x_c^-) lead to ferroptosis impairs to synthesize glutathione (GSH), which protects cells against ROS and lipid peroxidation (Wang et al., 2017). Consistently, erastin, an inhibitor of system x_c^-, induce iron-dependent cell death via inhibition of cysteine uptake into

cells.It was reported that sorafenib, FDA-approved anti-cancer agent, also inhibits system x_c^- (Dixon et al., 2014). In addition, depleting the intracellular GSH pool by buthionine sulfoximine (BSO) sufficiently induces ferroptotic cell death. Glutathione peroxidase 4 (GPX4), a GSH-dependent enzyme, is shown to be a key inhibitor of ferroptosis to reduces lipid hydroperoxides. Indeed GPX4 overexpression suppresses the ferroptosis, whereas deletion of GPX4 results in cell death suggesting that GPX4 activity is indispensible to prevent ferroptosis (Imai et al., 2017). Conversely, ferroptosis is inhibited by a number of small molecule including ferrostatin-1 and liproxstatin-1, which might be used as therapeutics for degenerative disease in brain, kidney and other tissues (Cao et al., 2016). Iron chelator deferoxamine also inhibited eratsin-induced cell death.

Sestrin2, a highly conserved throughout evolution antioxidant protein, is strongly up-regulated (Essler et al., 2009) by a diversity of stresses including DNA damage, oxidative and energetic stress, and hypoxia (Kim et al., 2015a). Previously, we reported that Sestrin2 protects against galactosamine/lipopolysaccharide-induced acute fulminant hepatitis and acetaminophen-induced liver injury (Kim et al., 2017). It was well known that acetaminophen induces a cell death through GSH depletion (Kim, et al., 2017). Moreover, recently reported that acetaminophen-induced cell death is also associated with ferroptosis in primary hepatocytes (Lorincz et al., 2015). Despite the significance of Sestrin2 in the regulation of cellular homeostasis against stress in liver, it is not known whether Sestrin2 might be associated with iron overloads induced liver injury (Bogdan et al., 2016).

In this study, we sought to determine whether Sestrin2 expression is regulated by ferroptosis conditions and if so what is the role of Sestrin2 in the cytoprotection against lipid ROS. We found that Nrf2-ARE signaling pathway is required for the ferroptosis-induced Sestrin2 gene expression (Sun et al., 2016). In addition we established HepG2 cells stably

expressing Sestrin2 to identify the molecular mechanism involved. We found that Sestrin2 expression inhibits erastin, representative ferroptosis inducer,--induced cell death, ROS formation, malondialdehyde (MDA) formation, GSH depletion and GPX4 reduction. Moreover, iron accumulation by erastin was inhibited by Sestrin2. These results indicate that up-regulated Sestrin2 expression under ferroptosis might be a potential therapeutic target in alleviating iron overloads-induced hepatotoxicity via regulating oxidative stress to reduce hepatocyte injury.

II. MATERIALS AND METHODS

1. Reagents and Antibodies

Antibodies against Nrf2, Lamin A/C were provided by Santa Cruz Biotechnology (Santa Cruz, CA). Sesn2 antibody was obtained from proteinteck (Chicago, IL). Horseradish peroxidase-conjugated anti-rabbit and anti-mouse antibodies, Mito SOX were purchased from Invitrogen (Carlsbad, CA). Erastin and Sorafenib were obtained from Selleck Chemicals (Houston, TX). 2', 7'-dichlorofluorscein siacetate (DCFH-DA), 3-(4,5-dimethylthiazol-2-yl)-2,5-diphenyl-tetrazolium bromide (MTT), Dimethylsulfoxide (DMSO), butylated hydroxyanisole (BHA), N-acetyl-L-cysteine (NAC), diphenyleneidonium chloride (DPI), actinomycin-D (ActD), L-Buthionine-sulfoximine (BSO), Ferrostatin-1 (Fer-1), Deferoxamine mesylate salt (DFO), ZVAD-FMK, and β-actin antibody were purchased from Sigma Chemicals (St. Louis, MO).

2. Cell culture

HepG2 and AML-12 cell lines were purchased from ATCC (Ametican Type Culture Collection, Manassas, VA). Nrf2 knockout and wild-type MEF cells were kindly donated by Dr. MK Kwak (Catholic University, Korea). AML-12 cells were cultured in 1:1 mixture of DMEM and Ham's F12 medium (Hyclone, Logan, UT) with 0.005 mg/mL transferring, and 5ng/mL selenium (Life Technologies, Gaithersburg, MD). HepG2 cells were maintained in DMEM containing 10% fetal bovine serum, 50 units/ml penicillin/ streptomycin at 37°C in a humidified 5% CO_2 atmosphere.

3. Establishment of a stable cell line expressing Sestrin2

Cells stably expressing Sestrin2 were established as previously described (Seo et al., 2015). HepG2 cells were transfected with the plasmid pCMV-Tag3A (mock-transfected) or pCMV-SESN2 by using Lipofectamine 2000 (Invitrogen, Carlsbad, CA) according to the manufacturer's instructions. After 1 day of transfection, colonies of geneticin-resistant cells were selected by treatment with geneticin (500 μg/mL) and then amplified in culture. Sestrin2 overexpression was established by immunoblotting.

4. Primary hepatocyte isolation

Primary hepatocytes were isolated and cultured as described previously (Seo, et al., 2015). Briefly, ICR mice were anesthetized with Zoletil (Virbac, France), and the portal vein was cannulated under aseptic conditions. The liver was perfused *in situ* with Ca^{2+}-free Hank's balanced saline solution (HSBB) at 37℃ for 5 min. Livers were then perfused for 20 min with HBSS containing 0.05% collagenase and Ca^{2+} at a flow rate 10 ml/min. After perfusion, the livers were minced gently with scissors and suspended in sterilized PBS. The cell suspension was then filtered through a cell strainer and centrifuged at 50 × g for 5 min to separate parenchymal and non-parenchymal cells. The viability of hepatocytes were plated on collagen-coated plates and cultured in DMEM containing 50 U/ml penicillin, 50 μg/ml streptomycin and 10% FBS, isolated hepatocytes were plated on collagen-coated plate and cultured in DMEM containing 50 units/ml penicillin and 50 μg/ml streptomycin with 10% FBS.

5. MTT assay

The measure cytotoxicity, HepG2 cells were plated at a density of 1 x 10^9 cells/well in 12 well plates and incubated with erastin (10 μM) for 24 h. After treatment, viable cells were stained

with MTT (0.2 mg/mL and incubated for 1 h). The media were then removed and any formazan crystals produced in the wells were dissolved with the addition of 300 μL of dimethyl sulfoxide. Absorbance at 550 nm was measured using an enzyme-linked immunosorbent assay microplate reader (spectra MAX, Molecular Device, Sunnyvale, CA). Cell viability was defined relative to the untreated control [i.e., viability (% control) = 100 x (absorbance of treated sample) / (absorbance of control)].

6. RNA isolation and RT-PCR analysis

Total RNA was extracted using Trizol (Invitrogen, Carlsbad. CA) according to the manufacturer's instructions. To obtain cDNA, total RNA (1 μg) was reverse-transcribed using an oligo (dT) 16 primer. The cDNA was amplified using a high capacity cDNA synthesis kit (Bioneer, Daejeon, Korea). PCR was conducted using a PCR premix (Bioneer Daejeon, Korea) with a thermal cycler (Bio-Rad, Hercules, CA). Primers were synthesized by Bioneer. The following primer sequences were used: human SESN1 sense 5'-CTTCTGGAGGCAGTTCAAGC-3' and antisense 5'-TGAATGGCAGCCTGTCTTCA-3'; human SESN2 sense 5'-CTCACACCATTAAGCATGGAG-3' antisense 5'-CAAGCTCGGAATTAATGTGCC-3'; human GAPDH sense 5'-GAAGATGGTGATGGGATTTC-3' and antisense 5'-GAAGGTGAAGGTCGGAGTC-3'; mouse SESN1 sense 5'-GGACGAGGAACTTGGAATCA-3' and antisense 5'-ATGCATCTGTGCGTCTTCAC-3'; mouse SESN2 sense 5'-TAGCCTGCAGCCTCACCTAT-3' and antisense 5'-TATCTGATGCCAAAGACGCA-3'; mouse GAPDH sense 5'- TGCCCCCATGTTTGTGATG-3' and antisense 5'-TGTGGTCATGAGCCCTTCC-3'. Glyceraldehyde-3-phosphate dehydrogenase (GAPDH) was used as a reference gene for normalization.

7. Plasmid transfection and Luciferase assay

The human Sestrin2 promoter-driven luciferase reporter construct, pGCL-phSESN2, was kindly provided by RIKEN BRC through the National Bioresource Project of NEXT, Japan. The plasmid pCDNA-mNrf2, which encodes murine Nrf2, was a gift from Dr Yamamoto, and has been described, previously reported (Seo, et al., 2015). A deletion mutant of the ARE in the Sesn2 promoter-luciferase reporter plasmid (pGL3-phSESN2-ΔARE) was constructed as previously described (Shin et al., 2012). Firefly and Renilla luciferase activities in cell lysates were measured using the dual luciferase assay system (Promega) according to the manufacturer's instructions.

8. Immunoblot analysis

Cell lysates were prepared according to the previously published methods (Yang, et al., 2015). Sodium dodecyl sulfate (SDS)-polyacrylamide gel electrophoresis and immunoblot analyses were performed according to previously published procedures (Kim *et al.*, 2015b). Briefly, the cell lysates were separated using 7.5% gel electrophoresis, The protein were then electophoretically transferred to nitrocellulose membranes. After the membranes were blocked, they were incubated with primary antibody at 4 ℃ overnight and then incubated with a horseradish peroxidase-conjugated secondary antibody (Zymed Laboratories, San Francisco, CA). The immune reactive protein was visualized using an ECL chemiluminesence detection kit (Amersham Biosciences, Buckinghamshire, UK). β-actin was used as immunoblotting controls. Three separate experiments were performed with different lysates to confirm the changes in the protein levels.

9. siRNA Knockdown Experiment

Cells were transfected with non-targeting control siRNA (100 pmol/ml), siRNA directed against Nrf2 (100 pmol) (ON-TARGET plus SMART pool, Dharmacon Inc., Lafayette, CO) for 36 h using Lipofectamine 2000 according to the manufacturer's instructions.

10. Determination of GSH content

The GSH contents in the cells were quantified using a commercial GSH determination kit (BIOXYTECH GSH-400, Oxis International). Cells were plated onto 6 well dishes and chemical treatment. And then, scraped cells were lysed in buffer containing 5% metaphosphoric acid to precipitate proteins. After being centrifuged at 10,000 × g for 15 min, the supernatants were used to measure GSH concentration. Absorbance at 400 nm was measured using a microplate reader (Spectra MAX, Molecular Device, Sunnyvale, CA).

11. Measurement of ROS production

The level of hydrogen peroxide production was determined by measuring the increase in dihlorofluorescein fluorescence after with and without erastin (10 μM) at 37℃ for 2 h, then incubated with DCFH-DA at 37℃ for 1 h. The harvested by trypsinization and washed PBS. The intensity of the fluorescence in the cells was measured using a Flow-cytometry (Beckman). DCFH-DA fluorescence was used channel FITC-A.

12. Mito SOX fluorescence analysis

Detection of intracellular superoxide in HepG2 cell. Cells were treated with and without erastin (10 μM) at 37℃ for 2.5 h, then incubated with Mito SOX at 37℃ for 30 minutes.

The harvested by trypsinization and washed PBS. The intensity of the fluorescence in the cells was measured using a Flow-cytometry (Beckman). Mito SOX fluorescence was used channel FL2-A.

13. Iron assay

The relative iron concentration in cell lysate were RIPA lysis buffer (1M Tris; PH 7.5, NP-40, Sodium Deoxycholate, 1M NaCl, 0.5M EDTA in distilled water) assessed using the Iron Assay Kit (no.DIFE-250; BioAssay Systems) according to manufacturer's instructions.

14. Lipid peroxidation assay

The relative malondialdehyde (MDA) quantitation in cell lysates was assessed using TBARS assay kit (no. STA-330; CELL BIOLABS) according to manufacturer's instructions.

15. statistical analysis

One-way analysis of variance (ANOVA) was used to determine the significances of differences between treatment groups. The Newman-Keuls test was used to determine the significances of differences between multiple group means. Results are expressed as means ± SE.

III. RESULTS

1. Increased Sestrin2 expression levels during ferroptosis

First, we investigated Sestrin2 expression by ferroptosis inducers in HepG2 cells. We examined the time course of Sestrin2 expression in response to treatment with erastin (10 μM), BSO (30 μM) and sorafenib (1 μM), respectively (Fig 1A). Sestrin2 protein level was increased after 3-12 h of erastin, BSO and sorafenib treatment. In other hepatocyte-derived cell lines AML-12 and primary hepatocyte from mice, Sestrin2 induction was observed by treatment with erastin (Fig 1B and C). Erastin-induced ferroptosis was confirmed using the specific ferroptosis inhibitors ferrostatin-1 (Fer-1) and iron chelator deferoxamine (DFO), which significantly reversed erastin-treated Sestrin2 induction. In contrast, inhibitors of other forms of cell death, including ZVAD-FMK (an apoptosis inhibitor) and necrostatin-1 (a necroptosis inhibitor), failed to rescue erastin-induced Sestrin2 expression (Fig 1D). These results suggest that ferroptosis inducers up-regulated the Sestrin2 expression via accumulation of iron.

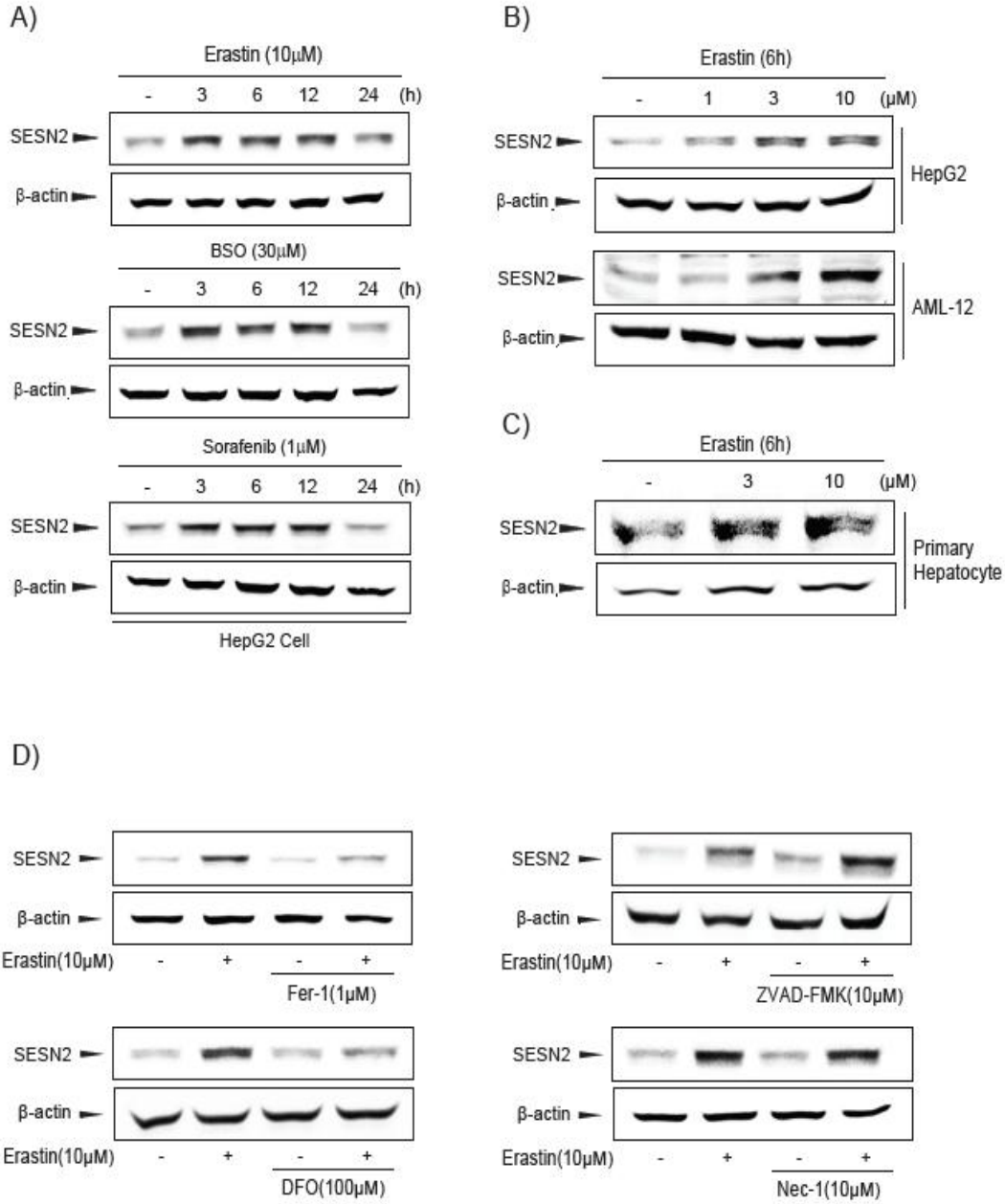

Figure 1. Increased Sestrin2 expression levels erastin-induced ferroptosis.

(A) Immunoblot analyses for Sestrin2 were carried out in cells treated with erastin (10 μM), BSO (30 μM) and sorafenib (1 μM) for 3-24 h. (B) The effect of varying concentrations of erastin on Sestrin2 induction in HepG2 and AML-12 cells. Sestrin2 protein was immunoblotted in the lysates of cells incubated with erastin (1, 3, 10 μM) for 6 h. (C) Immunoblot analyses for Sestrin2 were performed in primary hepatocytes with erastin for 6 h. (D) Immunoblot analyses for HepG2 cell were treated with erastin (10 μM) with or without indicated inhibitors for 6 h.

2. Transcriptional regulation of Sestrin2 expression

RT-PCR analysis was carried out to determine whether erastin-induced Sestrin2 expression was due to increased transcription. The results showed that Sestrin2 mRNA levels were increased by erastin treatment (Fig 2A). A reporter gene analysis of the sestrin2 promoter was performed in HepG2 cells transfected with a luciferase reporter construct containing the Sestrin2 promoter region (Fig 2B). Consistently, exposure of transfected cells to erastin significantly increased luciferase activity of pGL4-phSESN2. When the cells were pretreated with the transcription inhibitor actinomycin-D (ActD) for 30 minute before adding the erastin, and then the levels of Sestrin2 protein were measured. ActD treatment completely inhibited the increase in Sestrin2 levels induced by erastin (Fig 2C), which suggests that upregulation of Sestrin2 by erastin was due to increased transcription.

A)

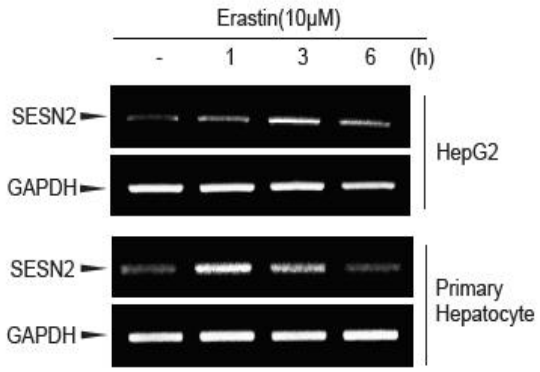

B)

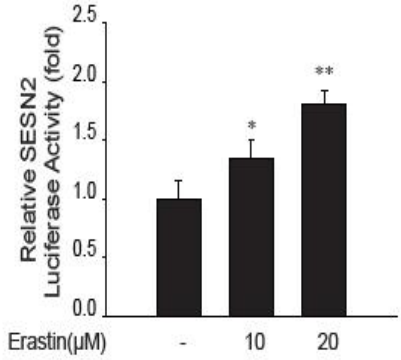

C)

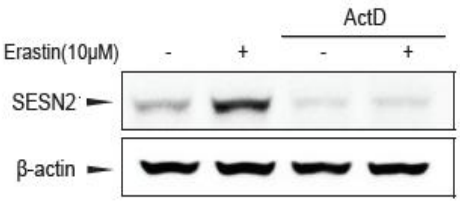

Figure 2. Transcriptional regulation of Sestrin2 expression

(A) RT-PCR analysis. Cells were treated with erastin (10 μM) for 1-6 h. Sestrin2 transcript levels were determined by RT-PCR using GAPDH used as an internal control. (B) Sestrin2-luciferase activity was determined in the lysates of HepG2 cells treated with erastin (10, 20 μM) for 12 h. Data represent the mean ± S.E. of three replicates; *P <0.05, **P<0.01, significant versus vehicle-treated control. (C) The effect of actinomycin-D (ActD) on Sestrin2 transcriptional regulation by erastin (10 μM) in HepG2 cells. The cells were treated with ActD (5 μg/ml) with or without erastin (10 μM).

3. Involvement of ROS production in erastin-induced Sestrin2 upregulation

Previously, we found that Sestrin2 is induced by oxidative stress and knockdown of Sestrin2 promoted cell death mediated by hydrogen peroxide (Kim, et al., 2015a). In addition, Sestrin2 has been shown to have cytoprotective activity against oxidative stress in various tissues. Therefore, we investigated whether overproduction of ROS under erastin-induced ferroptosis could lead to the induction of Sestrin2. First, we measured intracellular ROS accumulation by using DCFH-DA. When we treated with erastin (10, 20 μM) in HepG2 cells for 3 h, increase in intracellular ROS levels was observed (Fig 3A). To establish the induction of *Sestrin2* gene by ROS, we treated erastin (10 μM) in HepG2 cells for 6 h after pretreatment with antioxidant, such as BHA, NAC and DPI for 30 minutes. Antioxidants treatment completely inhibited the increase in Sestrin2 expression induced by erastin (Fig 3B). We checked three important signaling events in triggering ferroptosis which are depletion GSH, lipid peroxidation and iron accumulation (Fig 3C-E). In particular, ferrous iron (Fe^{2+}) participates in the fenton reaction, resulting in the generation of reaction of ROS, which goes on to trigger ferroptosis. Intracellular Fe^{2+} levels were significantly increased in erastin-treated hepatocytes.

A)

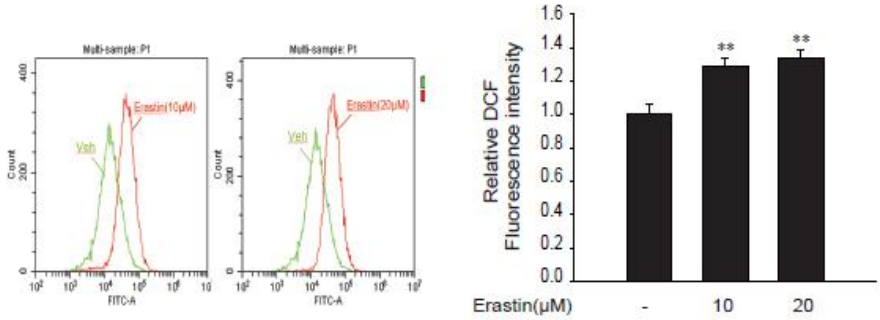

B)

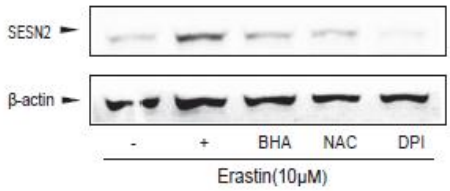

C)

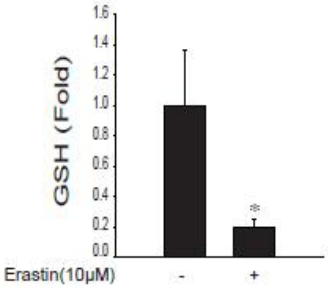

D)

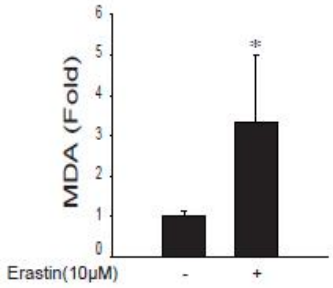

E)

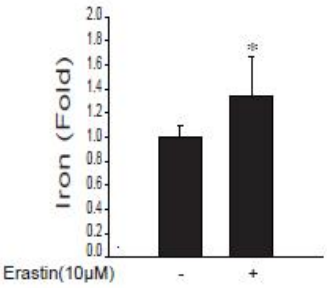

Figure 3. Involvement of ROS in erastin-induced ferroptosis

(A) ROS production by erastin in HepG2 cells. We measured fluorescence intensities using DCFH-DA after treated with erastin (10, 20 μM) for 3 h. Data represent means ± S.E. of three replicates. (B) HepG2 cells were exposed to erastin (10 μM) for 6 h after pretreatment with butylated hydroxyl anisol (BHA, 100 μM), N-acetyl-L-cysteine (NAC, 5 mM), and diphenyl eneidonium chloride (DPI, 1 μM) for 30 min. Sesetrin2 protein levels in lysates were measured by immunoblotting. (C-E) Indicated HepG2 cells were treated with erastin (10 μM) for 24 h. GSH (C), MDA (D) and Fe^{2} (E) levels were measured. Data represent the mean ± S.E. of three replicates; *P <0.05, **P<0.01, significant versus vehicle-treated control.

4. The role of Nrf2 activation in Sestrin2 induction by ferroptosis

Previously, we demonstrated that the Nrf2-ARE pathway is required for *sestrin2* gene expression, and it might protect cells against oxidative stress (Shin, et al., 2012). ARE luciferase constructs that containing a 3-tandem repeats sequence of ARE in the 5'-upstream region of NQO1 was transfected into cells to examine transactivating effect by erastin. Treatment with erastin resulted in a significant increase in luciferase activity of NQO1-ARE reporter gene construct (Fig. 4A). Next, we treated HepG2 cells with erastin at a concentration of 10 μM and then examined the effect of erastin on the nuclear accumulation of Nrf2. Treatment with erastin increased nuclear Nrf2 levels after just 30 minutes (Fig 4B). To examine the regulatory role of Nrf2-ARE on Sestrin2 promoter activity, we deleted the ARE site in the Sestrin2 promoter. Deletion of the ARE in the Sestrin2 promoter gene completely inhibited the erastin-induced increase in luciferase activity (Fig 4C). By transient expression of a specific siRNA directed against Nrf2, Sestrin2 expression was reduced in the treasfected cells. Nrf2 knockdown was confirmed by immunoblot analysis (Fig 4D). In a subsequent experiment using Nrf2 KO cells, we found that Nrf2 deficiency completely abolished erastin-induced Sestrin2 expression. These data indicate that Nrf2 activation is required for erastin-mediated Sestrin2 induction.

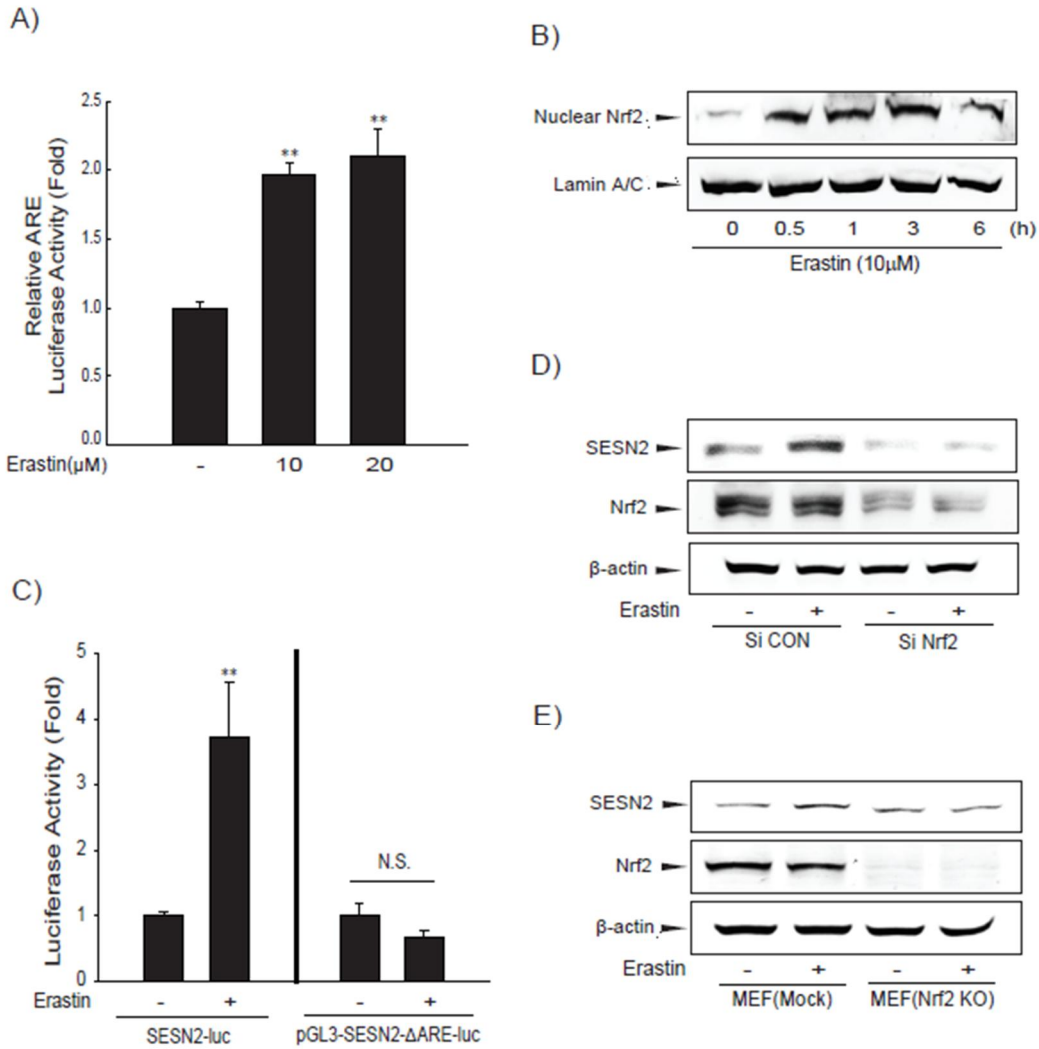

Figure 4. Involvement of Nrf2 activation in erastin-induced Sestrin2 induction

(A) Increases in Nrf2 transactivation by erastin. ARE luciferase assays were measured on the lysates of HepG2 cells transfected with the ARE luciferase construct exposed to erastin for 12 h. (B) HepG2 cells were treated with erastin (10 μM) for the indicated time, and Nrf2 translocation into the nucleus was then analyzed by immunoblotting. (C) Dual luciferase reporter assays were carried out with the lysates of HepG2 cells that had been transfected with pGL3-phSesn2 or pGL3-phSesn2-ARE (deletion mutant of ARE in Sestrin2). Reporter gene activities were calculated as a change in the ratio of firefly luciferase activity to Renilla luciferase activity. Data represent the mean ± S.E. of three replicates; **P<0.01, significant versus vehicle-treated control. (D) Effect of Nrf2 knockdown on Sestrin2 induction by erastin. HepG2 cells were transfected with control (CON) siRNA or Nrf2 siRNA for 36 h, and then treated with erastin (10 μM) for 6 h. (E) The effect of erastin on Sestrin2 induction in wild type (WT) and Nrf2 knockout (KO) MEF cells. Sestrin2 levels in the lysates of WT or Nrf2 KO cells treated with erastin (10 μM) for 3 h were examined by immunoblotting.

5. The cytoprotective effect of Sestrin2 against ferroptosis

To determine the role of Sestrin2 on erastin-induced ferroptosis, we generated stable cell line expressing Sestrin2 in HepG2 cells. Cell viability was assessed colorimetric MTT assay. The cell death of control cells is increased by erastin, whereas expressing Sestrin2 inhibited cell death. (Fig 5A). Next, we found that erastin-induced ROS was diminished in cells expressing Sestrin2 (Fig 5B). Moreover, mitochondrial ROS production was also inhibited by Sestrin2 expression as evidenced by experiment with mitochondria-targeted probes MitoSox (Fig 5C). Ferroptosis is characterized by the accumulation of lipid peroxidation. The end products of lipid peroxidation such as MDA were significantly decreased in cells expressing Sestrin2. GSH depletion and GPX4 reduction by erastin were reversed by Sestrin2 expression. Finally we found that iron accumulation by erastin was significantly inhibited in cells expressing Sestrin2 compare with control cells. These results indicate that Sestrin2 inhibited erastin-induced ferroptosis in hepatocytes through attenuation of iron accumulation and ROS formation.

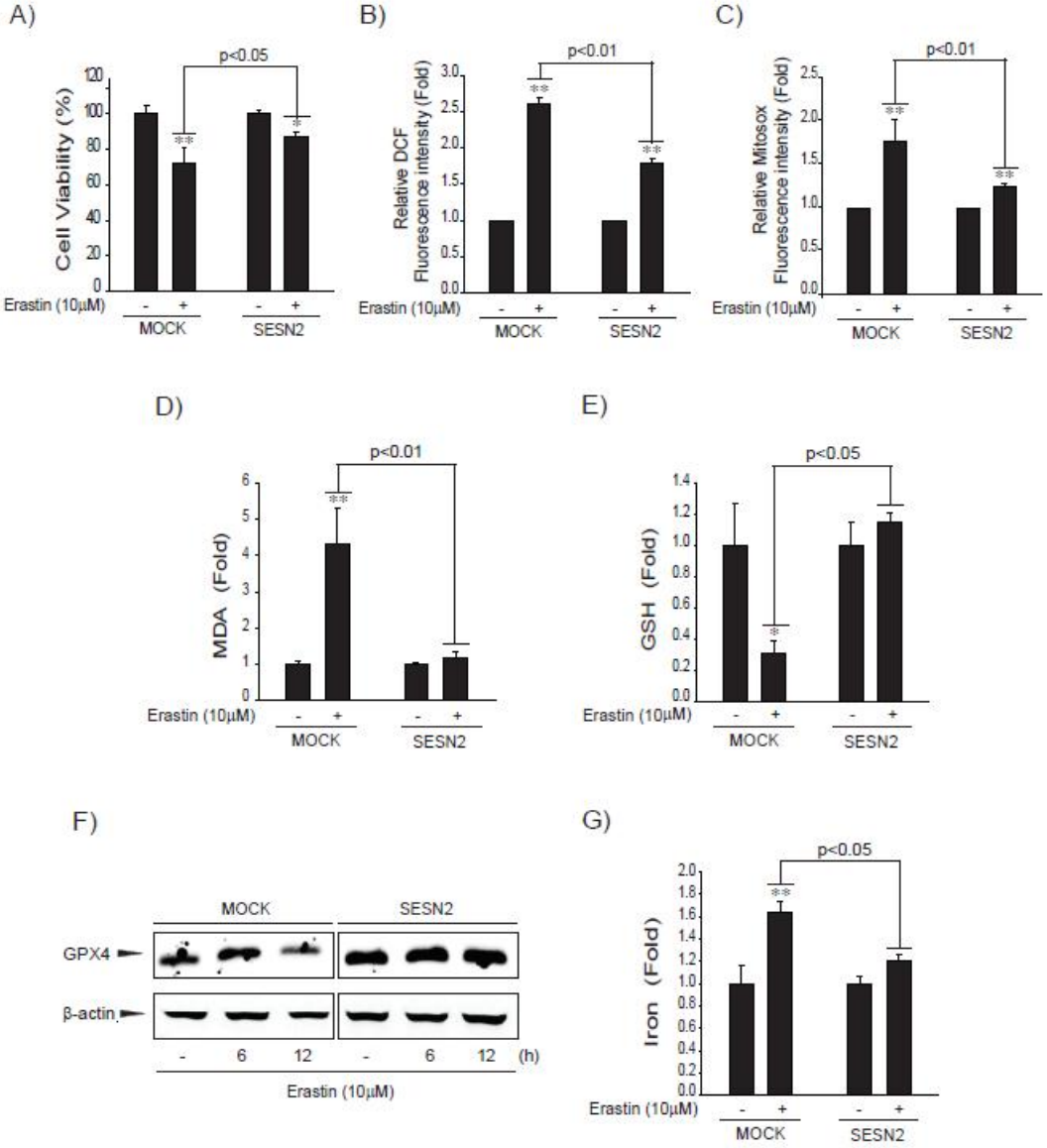

Figure 5. Sestrin2 overexpression inhibits erastin-induced ferroptosis

(A) The effect of Sestrin2 on erastin-induced cytotoxicity. Cells were treated with erastin (10 μM) for 24 h. Cell viabilities were assessed using an MTT assay. (B) Effect of Sestrin2 on erastin-induced ROS production. Cells were stained with 1 μM DCFH-DA for 1 h at 37°C. Intracellular fluorescence intensities were measured using a flow-cytometry analysis. (C) Mitochondrial production of ROS was determined by the use of the mitosox probe in control and Sestrin2 cells exposed to erastin (10 μM) for 3 h. (D) Lipid peroxidation is measured in the form of TBARS assay in cells exposed to erastin (10 μM) for 24 h. (E) The GSH concentration was measured in lysates of cells treated with erastin for 24 h. (F) Immunoblot analyses for GPX4 were carried out in cells treated with erastin (10 μM) for 6-12 h. (G) The level of iron was measured in cells exposed to erastin (10 μM) for 24 h. Data represent the mean ± S.E. of three replicates; * $P < 0.05$, ** $P < 0.01$, significant versus vehicle-treated control.

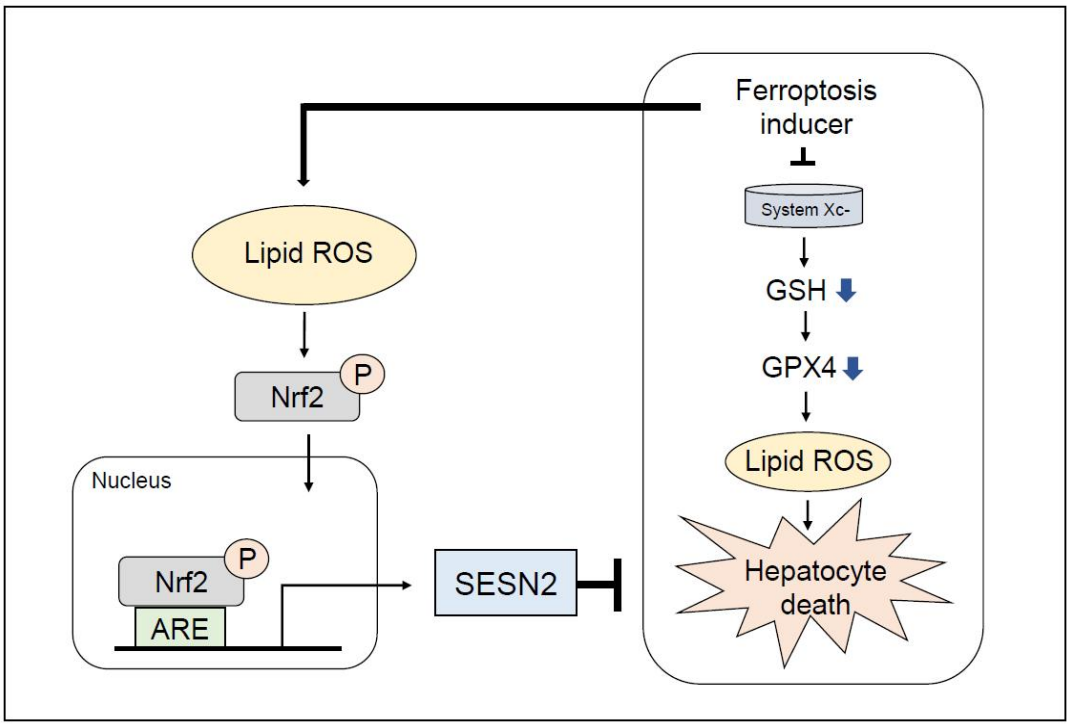

Figure 6. Schematic diagram of ferroptosis-induced Sestrin2 up-regulation inhibits iron overloads-mediated hepatocytes damage

IV. DISCUSSION

As shown several studies in patients with liver diseases are much more likely to have iron overload (Bogdan, et al., 2016). Recently proposed that ferroptosis occurred in mice liver fed with a high-iron diet and in genetic knockout mouse that develop severe iron overload (Prieto *et al.*, 1974). In addition, iron overload–induced liver damage (Sengsuk *et al.*, 2014) was reversed by treatment with ferrostatin-1. Representative liver injury models such as acetaminophen overdoses and ischemia/reperfusion has been demonstrated to induce ferroptosis which were ameliorated by the ferroptosis inhibitors (Yang, et al., 2015; Kim, et al., 2017). These observations indicate that iron accumulation in the liver result in ferroptotic cell death to liver injury (Lorincz, et al., 2015). Recently we suggest that Sestrin2, novel antioxidant protein, can maintain cellular homeostasis to reduce a series of stress (Essler, et al., 2009).

In the present study, we first identified the regulatory role of Sestrin2 in ferroptosis-mediated hepatocyte damage in cells. Stimulation of hepatocytes with ferroptosis inducers such as erastin, BSO and sorafenib elevates the up-regulation of Sestrin2, which depends on Nrf2 activation. Erastin-induced Sestrin2 expression was almost completely inhibited by only specific ferroptosis inhibitor or iron chelator, but not apoptosis or necroptosis inhibitor (Figure 1D). These results Sestrin2 up-regulation by erastin was due to iron accumulation and lipid ROS produced. We observed that treatment with ActD completely blocked the sestrin2 increase by erastin (Figure. 2C). Which indicate that the elevation in Sestrin2 expression by erastin was transcriptionally regulated.

We previously reported that Nrf2 is an essential transcription factor for Sestrin2 expression. Sestrin2 promoter contains ARE site, which is located in the proximal region of

promoter, from −550 to −539 bp (Shin, et al., 2012). Glucose deprivation (Seo, et al., 2015) and LPS (Yang, et al., 2015)-mediated Sestin2 expression required Nrf2 activation. These observations indicate that Nrf2-ARE pathway is essential for LPS-mediated Sestrin2 expression. Erastin increased translocation of Nrf2 from the cytosol into the nucleus and ARE-driven luciferase gene activity in hepatocytes. In addition, Nrf2 deficiency completely blocked the capability of erastin to increase Sestrin2 expression in Nrf2 knockout MEF cells. Moreover, a specific deletion of the ARE in the promoter region of the *Sestrin2* gene diminished luciferase activity by treatment with erastin (Fig XX). These results indicate that Nrf2-ARE signaling pathway is crucial for erastin-mediated Sestrin2 expression. However, it is also possible that Sestrin2 increases Nrf2 activity through the p62-dependent autophagic degradation of Keap1 (Bae *et al.*, 2013). Further study is still required whether up-regulation of Sestrin2 by ferroptosis condition protects cell through Sestrin2-mediated Nrf2 activation. It was recently reported that Nrf2 activation functions as an anti-ferroptosis. Ferroptosis inducers increased association p62 and Keap1 to displace Nrf2, thus inhibiting Nrf2 degradation (Sun, et al., 2016). Conversely, knockdown of Nrf2 and Nrf2-targete genes increased ferroptosis-inducing compounds-mediated cell death.

Furthermore, ferroptosis-mediated Sestrin2 expression prevented erastin-induced cell death by inhibiting ROS and MDA production, GSH depletion and GPX4 decrease which are main characteristics of ferroptosis (Xie, et al., 2016). Mitochondrial ROS production by erastin was also inhibited by Sestrin2 expression although some of the reports showed that mitochondrial ROS was not changed by erastin treatment (Figure 5C). This discrepancy might be due to the fact that different cell lines might have different cellular responses. These results indicate that Sestrin2 inhibited erastin-induced ROS production and lipid peroxidation production and consequent cell death.

Here, we found that iron accumulation by erastin was significantly inhibited by Sestrin2 expression (Figure 5G). Regulation of iron levels is sophisticatedly orchestrated. In the condition of iron deficiency, iron absorption is increased. Iron absorption regulated by hepcidin a hormone produced in the liver (Ganz *et al.*, 2012). In response to iron, hepcidin is secreted and thus plays as a negative feedback loop that limits iron absorption and retains iron in stores (Fung *et al.*, 2013). Hepcidin binds to the iron export basolateral transporter ferroportin which result in internalization and degradation by lysosomes and consequently reduced cellular iron export (De Domenico *et al.*, 2006). Further study is still required to decrease in iron accumulation by Sestrin2 expression is due to change in iron metabolism-mediated genes like hepcidin or ferroportin.

Collectively, our present results suggest that up-regulation of Sestrin2 expression by feroptosis-inducing compounds acts as a compensatory response for survival, inferring that Sestrin2 might be a promising therapeutic target for the iron over loads or ferroptosis associated liver diseases.

V. REFERENCES

1. Abbaspour, N., Hurrell, R., and Kelishadi, R. (2014). Review on iron and its importance for human health. J Res Med Sci **19**(2), 164-174.

2. Bae, S. H., Sung, S. H., Oh, S. Y., Lim, J. M., Lee, S. K., Park, Y. N., Lee, H. E., Kang, D., and Rhee, S. G. (2013). Sestrins activate Nrf2 by promoting p62-dependent autophagic degradation of Keap1 and prevent oxidative liver damage. Cell Metab **17**(1), 73-84.

3. Blumberg, J. (2004). Use of biomarkers of oxidative stress in research studies. J Nutr **134**(11), 3188S-3189S.

5. Bogdan, A. R., Miyazawa, M., Hashimoto, K., and Tsuji, Y. (2016). Regulators of Iron Homeostasis: New Players in Metabolism, Cell Death, and Disease. Trends Biochem Sci **41**(3), 274-286.

6. Cao, J. Y., and Dixon, S. J. (2016). Mechanisms of ferroptosis. Cell Mol Life Sci **73**(11-12), 2195-2209.

7. De Domenico, I., Ward, D. M., Musci, G., and Kaplan, J. (2006). Iron overload due to mutations in ferroportin. Haematologica **91**(1), 92-95.

8. Deugnier, Y., and Turlin, B. (2011). Pathology of hepatic iron overload. Semin Liver Dis **31**(3), 260-271.

9. Dixon, S. J., Patel, D. N., Welsch, M., Skouta, R., Lee, E. D., Hayano, M., Thomas, A. G., Gleason, C. E., Tatonetti, N. P., Slusher, B. S., et al. (2014). Pharmacological inhibition of cystine-glutamate exchange induces endoplasmic reticulum stress and ferroptosis. Elife **3**, e02523.

10. Essler, S., Dehne, N., and Brune, B. (2009). Role of sestrin2 in peroxide signaling in macrophages. FEBS Lett **583**(21), 3531-3535.

11. Fung, E., and Nemeth, E. (2013). Manipulation of the hepcidin pathway for therapeutic purposes. Haematologica **98**(11), 1667-1676.

12. Ganz, T., and Nemeth, E. (2012). Hepcidin and iron homeostasis. Biochim Biophys Acta **1823**(9), 1434-1443.

13. Horowitz, M. P., and Greenamyre, J. T. (2010). Mitochondrial iron metabolism and its role in neurodegeneration. J Alzheimers Dis **20 Suppl 2**, S551-568.

14. Imai, H., Matsuoka, M., Kumagai, T., Sakamoto, T., and Koumura, T. (2017). Lipid Peroxidation-Dependent Cell Death Regulated by GPx4 and Ferroptosis. Curr Top Microbiol Immunol **403**, 143-170.

15. Kim, K. M., Yang, J. H., Shin, S. M., Cho, I. J., and Ki, S. H. (2015a). Sestrin2: A Promising Therapeutic Target for Liver Diseases. Biol Pharm Bull **38**(7), 966-970.

16. Kim, M. G., Yang, J. H., Kim, K. M., Jang, C. H., Jung, J. Y., Cho, I. J., Shin, S. M., and Ki, S. H. (2015b). Regulation of Toll-like receptor-mediated Sestrin2 induction by AP-1, Nrf2, and the ubiquitin-proteasome system in macrophages. Toxicol Sci **144** (2), 425-435.

17. Kim, S. J., Kim, K. M., Yang, J. H., Cho, S. S., Kim, J. Y., Park, S. J., Lee, S. K., Ku, S. K., Cho, I. J., and Ki, S. H. (2017). Sestrin2 protects against acetaminophen -induced liver injury. Chem Biol Interact **269**, 50-58.

18. Latunde-Dada, G. O. (2017). Ferroptosis: Role of lipid peroxidation, iron and ferriti nophagy. Biochim Biophys Acta **1861**(8), 1893-1900.

19. Lorincz, T., Jemnitz, K., Kardon, T., Mandl, J., and Szarka, A. (2015). Ferroptosis is Involved in Acetaminophen Induced Cell Death. Pathol Oncol Res **21**(4), 1115-21. Miller, J. L. (2013). Iron deficiency anemia: a common and curable disease. Cold Sprin g Harb Perspect Med **3**(7).

20. Prieto, J., Barry, M., and Sherlock, S. (1974). Proceedings: Serum ferritin in patient s with iron overload and with acute and chronic liver disease. Gut **15**(4), 343.

21. Sengsuk, C., Tangvarasittichai, O., Chantanaskulwong, P., Pimanprom, A., Wantaneey awong, S., Choowet, A., and Tangvarasittichai, S. (2014). Association of Iron Overload with Oxidative Stress, Hepatic Damage and Dyslipidemia in Transfusion-Dependent beta-Thalassemia/HbE Patients. Indian J Clin Biochem **29**(3), 298-305.

22. Seo, K., Ki, S. H., and Shin, S. M. (2015). Sestrin2-AMPK activation protects mito chondrial function against glucose deprivation-induced cytotoxicity. Cell Signal **27**(7), 15 33-1543.

23. Shin, B. Y., Jin, S. H., Cho, I. J., and Ki, S. H. (2012). Nrf2-ARE pathway regula tes induction of Sestrin-2 expression. Free Radic Biol Med **53**(4), 834-841.

24. Sun, X., Ou, Z., Chen, R., Niu, X., Chen, D., Kang, R., and Tang, D. (2016). Acti vation of the p62-Keap1-NRF2 pathway protects against ferroptosis in hepatocellular car cinoma cells. Hepatology **63**(1), 173-184.

25. Wang, H., An, P., Xie, E., Wu, Q., Fang, X., Gao, H., Zhang, Z., Li, Y., Wang, X., Zhang, J., et al. (2017). Characterization of ferroptosis in murine models of hemoch romatosis. Hepatology **66**(2), 449-465.

26. Xie, Y., Hou, W., Song, X., Yu, Y., Huang, J., Sun, X., Kang, R., and Tang, D. (2 016). Ferroptosis: process and function. Cell Death Differ **23**(3), 369-379.

27. Yang, J. H., Kim, K. M., Kim, M. G., Seo, K. H., Han, J. Y., Ka, S. O., Park, B. H., Shin, S. M., Ku, S. K., Cho, I. J., et al. (2015). Role of sestrin2 in the regulation of proinflammatory signaling in macrophages. Free Radic Biol Med **78**, 156-167.